Supplementary Information

Cellular morphology and density control kinetic energy spectra in bacterial monolayer swarms

Xiao Chen,*[a] Ming Yuan,[b] Hepeng Zhang[b] and He Li*[b, c]

[a]*School of Life Science, Huaiyin Normal University, 223300 Huai'an, China. E-mail: chenxiao419@gmail.com*

[b]*Institute of Natural Sciences and School of Physics and Astronomy, Shanghai Jiao Tong University, 200240 Shanghai, China*

[c]*Institut de Génétique et de Biologie Moléculaire et Cellulaire, CNRS, Inserm, 67400 Illkirch, France. E-mail: liheg36ke@gmail.com*

1. Methods section

1.1 Experimental method

A small amount frozen stocks of Wild-type *Serratia marcescens* (ATCC 274) was first inoculated into 4 mL of Luria Broth liquid medium, and then incubated overnight at 30°*C* with shaking at 200 rpm. A 5 μL drop of overnight *S. marcescens* bacterial cultures (optical density OD650 ≈ 1.0) were inoculated at the center of 0.5% Eiken agar plate containing 25 g/L Luria Broth supplemented with 18 μg/mL Brij-35, an exogenous surfactant to form monolayer of cells at the front of colony by accelerating the expansion rate of bacteria, and antibiotic drug Cephalexin with various concentrations from 40 to 80 μg/mL to change the average cell length. The inoculated plates are incubated at 30°*C* and 90% humidity. The *S. marcescens* colony began expanding outwards in a branching pattern after a lag time of around 3 hours and swarmed with a front speed approximately 2.5 μm/s, only about 10% of the mean speed of isolated bacteria. We captured bacterial movement in the monolayer regions of varying area fractions within a window of 554 × 277 μm^2 through a 40× objective (Nikon S plan Fluor). Videos were recorded at 90 frame/s for 24 seconds, during which the total number of the bacteria remained almost unchanged, and the system is in a quasi-steady state.

3.2 Image analysis and cluster identification

Data analysis was conducted using custom MATLAB scripts. The bacterial velocity measured by particle tracking velocimetry was used to calculate the correlation function and the energy spectrum. Cell isolation and tracking followed the similar procedures as described previously[1]. We employed Particle Image Velocimetry (PIV) to measure the velocity field of dense bacterial populations to visualize the dynamical structures formed in the active turbulent state, and used the results to cross-validate the energy spectrum calculated via particle tracking at high density (Fig. S5). The software PIVLab[2] was used to calculate the velocity field, with the interrogation window size set to 32 × 32 $pixel^2$ (4.3 × 4.3 μm^2).

To identify clusters, two neighboring bacteria are defined to belong to the same cluster if their centers of mass are within a distance D and an angle deviation θ according to the method outlined in Ref. [1]. It is found that, at any density, the average angular difference between the body orientation of a bacterium and that of all its neighbors within a distance of half its cell length is less than 15°. Thus, we empirically choose θ = 15° and set D to be 80% of the average cell length at different area fractions to identify clusters (Fig. 1(d) and Video 1, ESI†).

3.3 Defect detection and analysis

To detect topological defects, we first computed the bacterial orientation field using the Structure Tensor Algorithm outlined in Ref. [3], an edge-feature recognition method based on grayscale gradients. As this algorithm requires sharp edges in the objects within the images, we initially enhanced the raw grayscale images with a Gaussian high-pass filter. Next, we smoothed the structure tensor of the sharpened grayscale field using a Gaussian filter with a width of 16 pixels (2.2 μm) and calculated the eigenvalues and eigenvectors at each pixel. The orientation of the local bacterial body was then given by the direction of the eigenvector with the smaller eigenvalue. Through this process, we extracted a reliable orientation field from each frame of the original video. To locate defects, we further smoothed the orientation field using a Gaussian filter with a 32 × 32 pixel^2 window to reduce noise. The orientation field was then interpolated onto a fine grid of 512 × 256, with a spatial resolution of 1.1 μm. For each grid point, the net change in director angle around a clockwise loop was computed. Points with a net orientation change of π (or −π) were marked as the core locations of +1/2 (or −1/2) defects.

To measure the velocity field near defects, the velocity vectors around isolated defects at different times and locations were counter-rotated in alignment with the defect orientation angle and subsequently superimposed into a unified reference frame. The ensemble-averaged velocity field was derived by averaging over 7630 positive defects and 7837 negative defects. An analogous procedure was employed to analyze area

fraction fluctuations. Local area fraction fluctuation fields around individual defects were rotated to align with the defect orientation, and then calculate the ensemble-average of the rotated fields.

2. Description of supplementary videos

We provide five videos for different dynamic states. Videos 1 shows bacteria in the clustering state with ϕ = 0.34, α = 8.4. Clusters are identified with instantaneous velocity vectors with random colors overlaid on bacteria. Video 2 shows instantaneous velocity field of bacteria in the active turbulent state with ϕ = 0.63, α = 6.4. Video 3 shows the bipolar motion of bacteria in the active nematic state. Video 4 shows the topological defects formed in the active nematic state with ϕ = 0.6, α = 9.2. All videos are played at 90 frames per second.

References

[1] X. Chen, X. Dong, A. Be'er, H. L. Swinney and H. Zhang, *Physical Review Letters*, 2012, 108, 148101.

[2] W. Thielicke and E. J. Stamhuis, *Journal of Open Research Software*, 2014.

[3] H. Li, X.-q. Shi, M. Huang, X. Chen, M. Xiao, C. Liu, H. Chate and H. P. Zhang, *Proceedings of the National Academy of Sciences*, 2019, 116, 777–785.

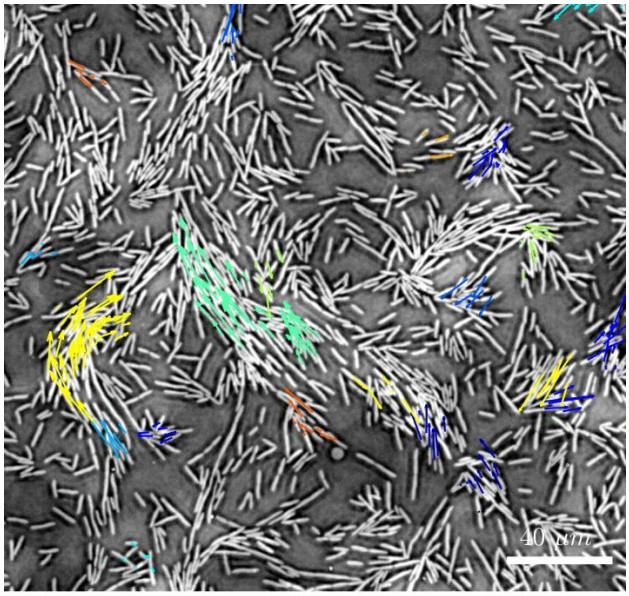

Fig. S1 Snapshot of monolayer bacterial swarms at $\phi = 0.17$, $\alpha = 8.2$. Instantaneous velocity vectors of bacteria, displayed in random colors for various clusters, are overlaid on a top-view experimental image.

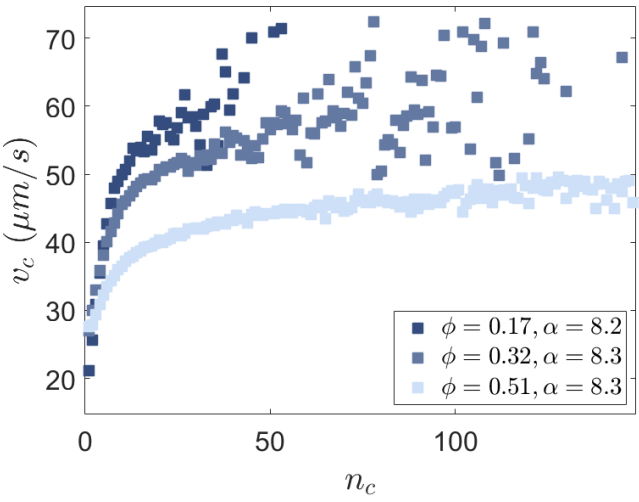

Fig. S2 the average velocity of bacteria within a cluster, v_c, increases with the cluster size, quantified by the number of bacteria within the cluster, n_c.

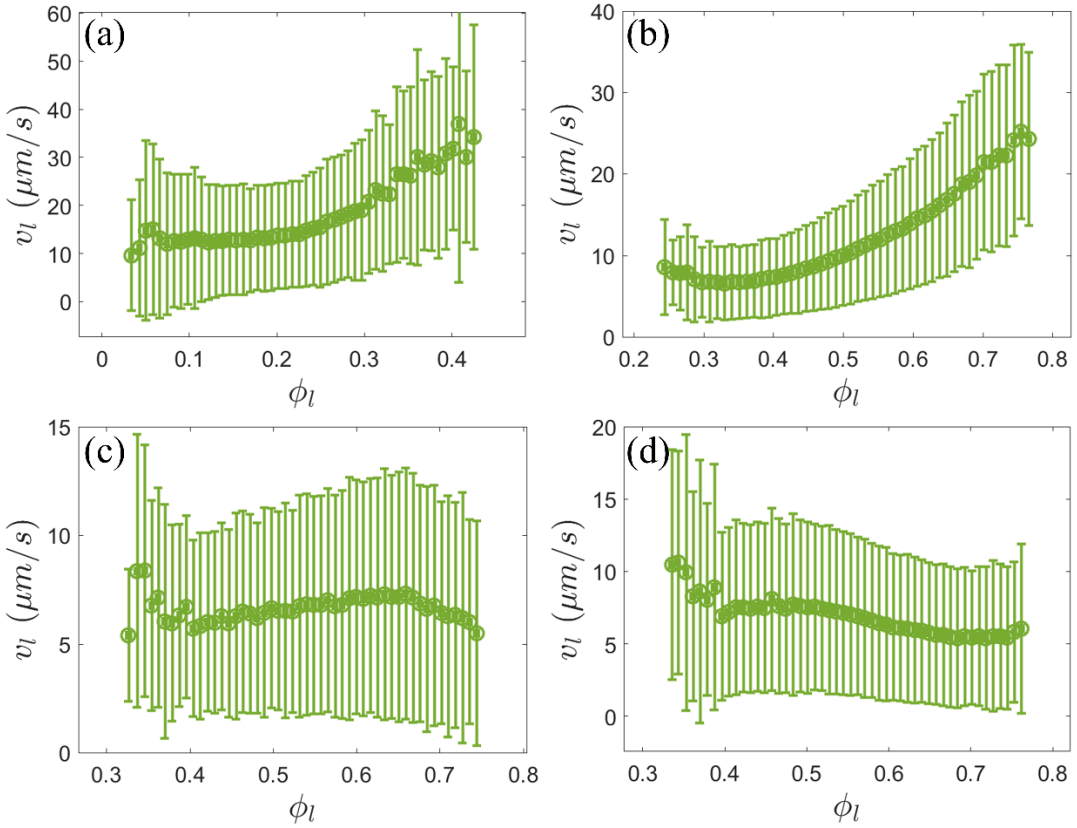

Fig. S3 The dependence of the local mean velocity v_l, measured within regions of size 17.3 × 17.3 μm^2, on the local area fraction ϕ_l at $\phi = 0.17$, $\alpha = 8.2$ (a), $\phi = 0.37$, $\alpha = 7.7$ (b), $\phi = 0.60$, $\alpha = 9.4$ (c) and $\phi = 0.63$, $\alpha = 9.6$ (d).

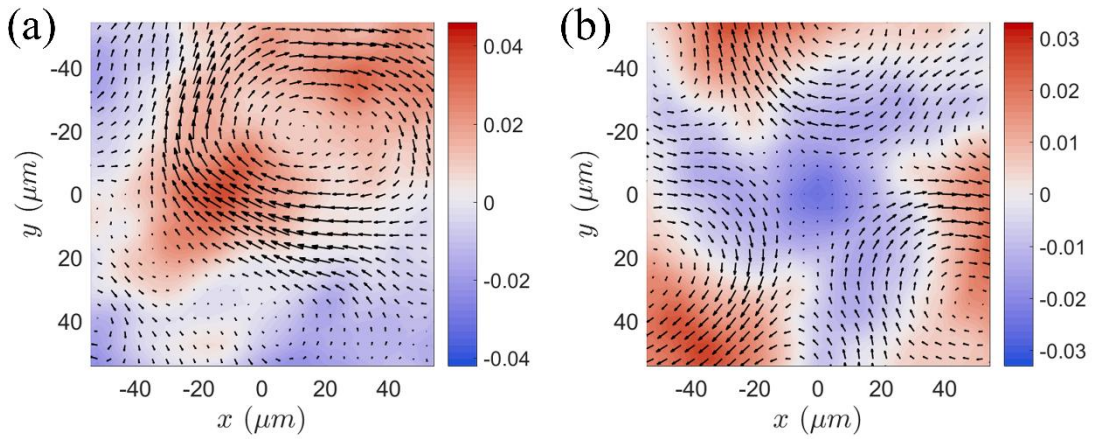

Fig. S4 Experimentally measured bacterial velocity field (black arrows) around+1/2 (a) and −1/2 (b) defect cores ($\phi = 0.60$, $\alpha = 9.2$), overlaid on the local area fraction fluctuations $\Delta\Phi(x, y)$ at the corresponding defects (red–blue color scale), defined as $\Delta\Phi(x, y) = \Phi(x, y) - \phi$, where $\Phi(x, y)$ and ϕ denote the local and global average area fractions, respectively.

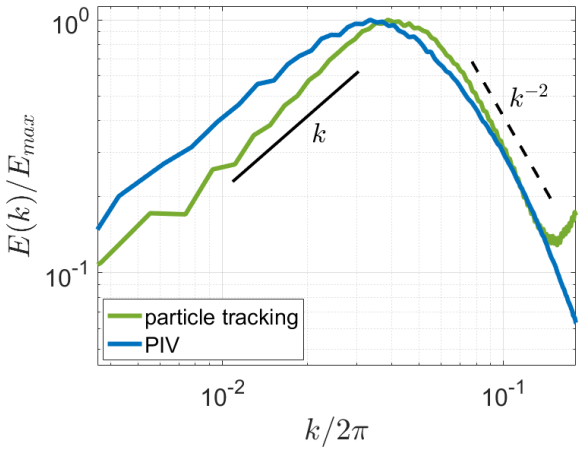

Fig. S5 The kinetic energy spectrum for ϕ = 0.63, α = 6.4 was measured separately using PIV (blue) and particle tracking velocimetry (green).